Available online at www.sciencedirect.com
ScienceDirect
Journal of Non-Crystalline Solids 354 (2008) 1080–1088
JOURNAL OF NON-CRYSTALLINE SOLIDS
www.elsevier.com/locate/jnoncrysol

Formation and properties of $RE_{55}Al_{25}Co_{20}$ (RE = Y, Ce, La, Pr, Nd, Gd, Tb, Dy, Ho and Er) bulk metallic glasses

S. Li, R.J. Wang, M.X. Pan, D.Q. Zhao, W.H. Wang *

Institute of Physics, Chinese Academy of Sciences, P.O. Box 603, 100080 Beijing, China

Received 19 September 2006; received in revised form 21 June 2007
Available online 19 September 2007

Abstract

We report that a series of ternary $RE_{55}Al_{25}Co_{20}$ (RE = Y, Ce, La, Pr, Nd, Gd, Tb, Dy, Ho and Er) alloys can be readily cast into bulk glasses by a conventional casting method. The characteristics and properties of these new bulk metallic glasses (BMGs) are studied and compared. Due to the chemical comparability and well-regulated variety in atomic size, properties and elastic constants of these rare earth elements, the $RE_{55}Al_{25}Co_{20}$ BMGs could be regarded as a model system to investigate the glass-forming ability, thermal stability, glass transition, crystallization behavior, liquid fragility, elastic and mechanical properties as well as their relationships. An attempt is made to highlight commonality and contrasts of the effects of various factors on the metallic glasses formation and properties.

PACS: 81.05.Kf; 61.43.Dq

Keywords: Amorphous metals; Metallic glasses

1. Introduction

Bulk metallic glasses (BMGs) have obtained considerable attention from both scientific and technological aspects in the past decades due to their excellent glass-forming ability (GFA) and many superior properties compared with their crystalline counterparts [1–3]. The GFA is often considered to be a dynamic competition between cooling rate and crystallization kinetics [4–6]. The high GFA means that the alloys can be vitrified in bulk form corresponding to the lower critical cooling rate R_c and the resulting glasses have a high resistance to crystallization process on its subsequent thermal exposure. The GFA can be quantitatively described by the value of R_c, but the R_c cannot be conveniently measured because of its susceptivity for cooling process. Therefore, various criteria and parameters have been proposed to predict and evaluate the GFA of an alloy [7–9]. These include reduced glass transition temperature T_{rg} ($T_{rg} = T_g/T_l$, where T_g and T_l are glass transition temperature and liquidus temperature, respectively), the temperature interval of the supercooled liquid region ΔT and γ ($\gamma = T_x/(T_g + T_l)$, where T_x is crystallization onset temperature). However, with the development of more and more new BMG systems, these criteria do not agree well with all experimental results. In fact, glass formation is a very complicated problem influenced by involved structural, thermodynamic and kinetic factors. The main factors that influence the GFA and the formation mechanism need to be explicitly elucidated.

Recently, more and more multi-component BMGs such as Fe-, Mg-, Sc-, Y-, Zr-, Pd-, Ln-(Ln = La, Ce, Pr, Nd, Sm, Gd, Tb, Dy, Ho and Er) and Cu-based alloy systems [1–4,10–13] were fabricated. This permits better review of the GFA, thermal stability, liquid fragility, elastic constants and mechanical properties: all are the key concerns for metallic glasses. The increasing experimental results have shown that there are correlations among these characteristics [14]. However, due to the variety and complexity of

* Corresponding author. Fax: +86 10 82640223.
E-mail address: whw@aphy.iphy.ac.cn (W.H. Wang).

0022-3093/$ - see front matter © 2007 Elsevier B.V. All rights reserved.
doi:10.1016/j.jnoncrysol.2007.08.022

Table 1
The atomic radius R, density ρ, melting temperature T_m, Poisson ratio σ and elastic constants (Young's modulus E, shear modulus G and bulk modulus B) of RE elements at room temperature

Element	E (GPa)	G (GPa)	B (GPa)	σ	H_v (GPa)	R (nm)	ρ (g/cm^3)	T_m (K)
Y	64	26	41	0.24	–	0.180	4.47	1783
La	37	14	28	0.28	4.91	0.188	6.15	1193
Ce	34	14	22	0.24	2.70	0.183	7.14	795
Pr	37	15	29	0.28	4.00	0.183	6.64	1208
Nd	41	16	32	0.28	3.43	0.182	6.80	1297
Sm	50	20	38	0.27	4.12	0.180	7.353	1345
Gd	55	22	38	0.26	5.70	0.180	7.90	1583
Tb	56	22	39	0.26	8.63	0.178	8.22	1629
Dy	61	25	41	0.25	5.40	0.177	8.55	1680
Ho	65	26	40	0.23	4.81	0.177	8.80	1734
Er	70	28	44	0.24	5.89	0.176	9.07	1770

the known BMGs, these correlations need to be further illuminated and validated. So it is of significance for exploiting a simple alloy system and reviewing these correlations in the model system.

Rare-earth (RE) elements have attracted standing attentions in the development of metallic glasses because of their chemical comparability, fantastic physical and chemical properties, which come from the unique configuration of unpaired 4f and 5f electrons and well-regulated changing atomic size, density and elastic constants (as shown in Table 1). In addition, RE elements have been found to be very effective for improving the GFA of an alloy [15] and RE-based alloys with good GFA have also been broadly reported [4,8,11,16–19]. Although lanthanide RE elements hold the same location in periodic table of the elements and have plenty of similar characteristics, RE-based BMGs show various GFAs and the size of the resultant glasses changes from thin ribbon to bulk form. Therefore, if a series of RE-based BMGs with the same composition can be synthesized, they are a potential model system for investigating the GFA and properties including thermal stability, fragility, elastic and mechanical properties. This kind of model system may useful for studying some fundamental issues in glass physics and material sciences.

In this paper, we report the formation of $RE_{55}Al_{25}Co_{20}$ (RE = Y, Ce, La, Pr, Nd, Sm, Gd, Tb, Dy, Ho and Er) BMGs. These alloys show various glass forming abilities, regularly increasing of thermal stability, Vicker's hardness H_v and fracture strength σ_f with the increase of elastic constants of the base RE elements and the strong liquid behavior. We have checked the validity of the known parameters for describing GFA and the established correlations in thermal stability, glass transition, crystallization behavior, liquid fragility, elastic and mechanical properties in these BMGs.

2. Experimental

The ingots of the alloys $RE_{55}Al_{25}Co_{20}$ with the nominal compositions listed in Table 2 were prepared by arc melting of the constituent elements La, Ce, Pr, Nd, Sm, Gd, Tb, Dy, Ho, Er, Y, with Al and Co in a Ti-gettered argon atmosphere. The ingots were remelted several times to ensure the homogeneity of the samples and then were suck-cast into copper molds with various inner diameters to obtain cylindrical rods. The structure of the samples was analyzed with X-ray diffraction (XRD) using a MAC M03 XHF diffractometer (CuK_α radiation). Thermal

Table 2
The composition of $RE_{55}Al_{25}Co_{20}$ BMGs, their glass transition temperature T_g, onset temperature of crystallization T_x and onset melting temperature T_m, liquidus temperature and glass-forming ability represented by a reduced glass transition temperature T_{rg}, $\Delta T = T_x - T_g$ and γ ($\gamma = T_x/(T_g + T_l)$) and critical diameter d_c

Composition	d_c (mm)	T_g (K)	T_x (K)	T_m (K)	T_l (K)	ΔT (K)	T_{rg} (K)	γ
$Y_{55}Al_{25}Co_{20}$	2	633	694	1035	1060	61	0.597	0.410
$La_{55}Al_{25}Co_{20}$	5	477	540	712	771	63	0.619	0.433
$Ce_{55}Al_{25}Co_{20}$	1	–	538	675	800	–	–	–
$Pr_{55}Al_{25}Co_{20}$	5	509	585	806	826	76	0.616	0.438
$Nd_{55}Al_{25}Co_{22}$	2	525	593	839	859	68	0.611	0.428
$Sm_{55}Al_{25}Co_{20}$	1	529	555	842	885	26	0.598	0.393
$Gd_{55}Al_{25}Co_{20}$	2	585	657	949	971	72	0.602	0.422
$Tb_{55}Al_{25}Co_{20}$	3	612	674	973	1001	62	0.611	0.418
$Dy_{55}Al_{25}Co_{20}$	3	635	708	998	1031	73	0.616	0.425
$Ho_{55}Al_{25}Co_{20}$	3	649	707	1035	1055	58	0.615	0.415
$Er_{55}Al_{25}Co_{20}$	5	663	722	1056	1079	59	0.628	0.414

Heating rate: 10 K/min.

properties were investigated in a Perkin–Elmer differential scanning calorimeter (DSC) DSC-7 and differential thermal analyzer (DTA) DTA-7 under a continuous argon flow. The values of T_g, T_x, melting temperature T_m and liquidus temperature T_l were determined from the thermal analysis traces with the accuracy of ±1 K. The acoustic velocities at ambient temperature were measured by using a pulse echo overlap method and the travel time of ultrasonic waves propagating through the sample with a 10 MHz frequency were obtained using a MATEC 6600 ultrasonic system with a measuring sensitivity of 0.5 ns [20]. The density ρ was determined by the Archimedean principle with an accuracy of 0.1%. Young's modulus E, bulk modulus B, shear modulus G and Poisson ratio σ were determined from the sound velocities and density as follow [21]: $G = \rho v_s^2, B = \rho(v_l^2 - 4/3v_s^2), \sigma = \rho(v_l^2 - 2v_s^2)/2(v_l^2 - v_s^2), E = 2G(1+\sigma)$, where v_l, v_s are longitudinal and transverse acoustic velocities, respectively. The Vicker's hardness H_v was measured with a Neophoto-21 micro-hardness tester at a load of 100 g. The value of compression fracture strength σ_f was obtained with the sample of 2 mm diameter on a servo-hydraulic materials testing system.

3. Results and discussion

3.1. The formation and GFA of $RE_{55}Al_{25}Co_{20}$ ternary BMGs

Fig. 1 presents the XRD patterns of the $RE_{55}Al_{25}Co_{20}$ alloys. For the samples below the critical diameters given in Table 2, except for $Ce_{55}Al_{25}Co_{20}$ and $Sm_{55}Al_{25}Co_{20}$ alloys, their XRD patterns exhibit a broad maximum in the range of $25° < 2\theta < 45°$ and the absence of any crystalline reflection indicative of glass formation. The typical DSC curves of these samples presented in Fig. 2(a) display a distinct endothermic characteristic of the glass transition and two or three sharp crystalline peaks further confirming

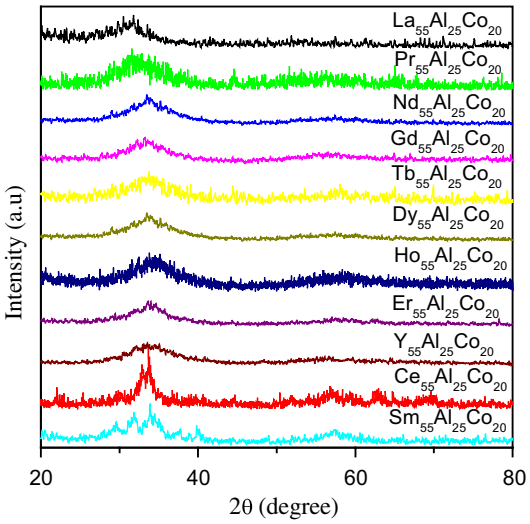

Fig. 1. XRD patterns of the as-cast $RE_{55}Al_{25}Co_{20}$ (RE = La, Ce, Nd, Pr, Sm, Gd, Tb, Dy, Ho, Er, Y) alloys.

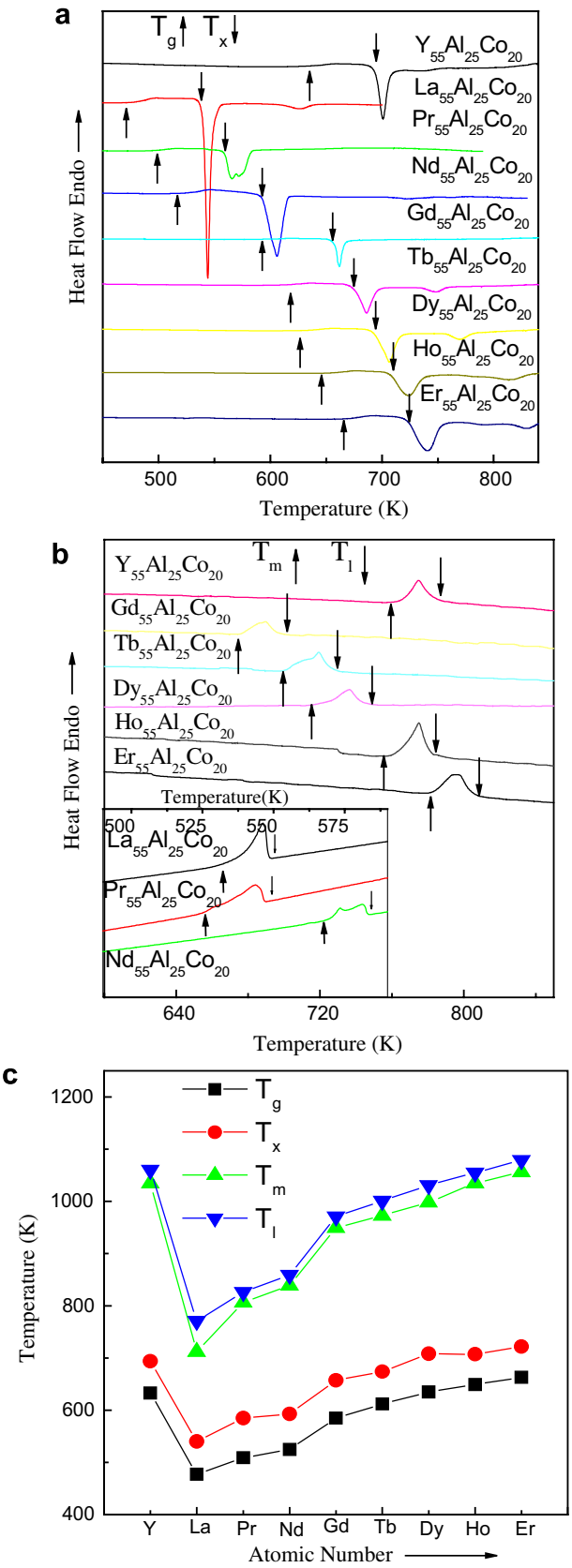

Fig. 2. (a) DSC curves of the as-cast $RE_{55}Al_{25}Co_{20}$ (RE = La, Nd, Pr, Gd, Tb, Dy, Ho, Er, Y) alloys. (b) DTA curves of the as-cast $RE_{55}Al_{25}Co_{20}$ alloys. (c) The dependence of T_g, T_x, T_m and T_l on the atomic number of RE element of the as-cast $RE_{55}Al_{25}Co_{20}$ alloys.

their amorphous structure. However, for $Ce_{55}Al_{25}Co_{20}$ and $Sm_{55}Al_{25}Co_{20}$ alloys with 1 mm diameter, XRD and DSC results indicate that they are only partial vitrified. Fig. 2(b) is DTA traces exhibiting the melting processes of these samples and the inset is DTA traces of $La_{55}Al_{25}Co_{20}$, $Pr_{55}Al_{25}Co_{20}$ and $Nd_{55}Al_{25}Co_{20}$ alloys with low melting temperature. The single endothermal signal corresponding to the melting process indicates that these ternary alloys are in eutectic composition point. While the $Ce_{55}Al_{25}Co_{20}$ and $Sm_{55}Al_{25}Co_{20}$ alloys show two or three endothermal signals indicating they are far from in eutectic composition point. This can explain why the two alloys have poor GFA.

As shown in Table 2 and Fig. 2(c), the $La_{55}Al_{25}Co_{20}$ alloy has the lowest T_g (477 K), while $Er_{55}Al_{25}Co_{20}$ alloy has the highest T_g (649 K) among these BMGs and the value of T_g increase gradually with the increasing of elastic moduli (especially for bulk modulus) of the RE element (as shown in Table 1). In addition, the T_x, T_m and T_l have also similar changing trend in these BMGs. This means that the thermal stability of the $RE_{55}Al_{25}Co_{20}$ BMGs can be tailored via the substitution of the base RE constituent with different elastic moduli. The $RE_{55}Al_{25}Co_{20}$ BMGs, with the broad values of T_g ranging from low temperature (close to room temperature) to high temperature (close to those of Zr- and Fe-based BMGs [1,3]), provide a useful system for investigating the glass transition, dynamic characteristics and relaxations.

Table 2 lists the critical diameter d_c (mm), T_{rg}, γ and ΔT of the $RE_{55}Al_{25}Co_{20}$ alloys. Although RE elements have similar physical and chemical characteristics, the GFA of the $RE_{55}Al_{25}Co_{20}$ alloys are obvious different. For $La_{55}Al_{25}Co_{20}$, $Pr_{55}Al_{25}Co_{20}$ and $Er_{55}Al_{25}Co_{20}$ alloys, the glassy rods can be obtained with the diameter of 5 mm and $Y_{55}Al_{25}Co_{20}$, $Gd_{55}Al_{25}Co_{20}$ and $Nd_{55}Al_{25}Co_{20}$ can only be fabricated with the diameter of 2 mm, while $Ce_{55}Al_{25}Co_{20}$ and $Sm_{55}Al_{25}Co_{20}$ cannot be obtained in bulk glassy form ($d_c \leqslant 1$ mm).

According to the formation criteria of BMGs [1,22], the adequate atomic radius difference, the large negative heat of mixing between the constituents and the eutectic composition can result in the excellent GFA of an alloy. To validate these criteria, Fig. 3 shows the relationship between R_c and the thermodynamic criteria (T_{rg}, γ and ΔT), electronegativity, the heat of mixing and atomic size difference. The R_c can be estimated by using: $dT/dt\,(K/s) = 10/d_c^2\,(cm)$ [23]. The γ and ΔT do not agree well with the GFA of these $RE_{55}Al_{25}Co_{20}$ alloys. For example, the R_c of $Er_{55}Al_{25}Co_{20}$ alloy is about 40 K/s and less than 250 K/s of $Nd_{55}Al_{25}Co_{20}$ alloy, but its ΔT (59 K) is smaller than that of $Nd_{55}Al_{25}Co_{20}$ alloy (68 K). The R_c of $Gd_{55}Al_{25}Co_{20}$ alloy with $\gamma = 0.422$. is about 250 K/s and much larger than 40 K/s of $Er_{55}Al_{25}Co_{20}$ alloy with $\gamma = 0.411$. The T_{rg} can adequately reflect the GFA of the $RE_{55}Al_{25}Co_{20}$ alloys as shown in Fig. 3. The heat of mixing ΔH^{mix}(RE–Al) and electronegativity of RE elements are similar and have no obvious correlation with the GFA of the $RE_{55}Al_{25}Co_{20}$ alloys. A large atomic size difference between the components is usually associated with the dense packing structure and the ease of glass formation [1–3]. For the $RE_{55}Al_{25}Co_{20}$ alloys, the differences in atomic radii of the

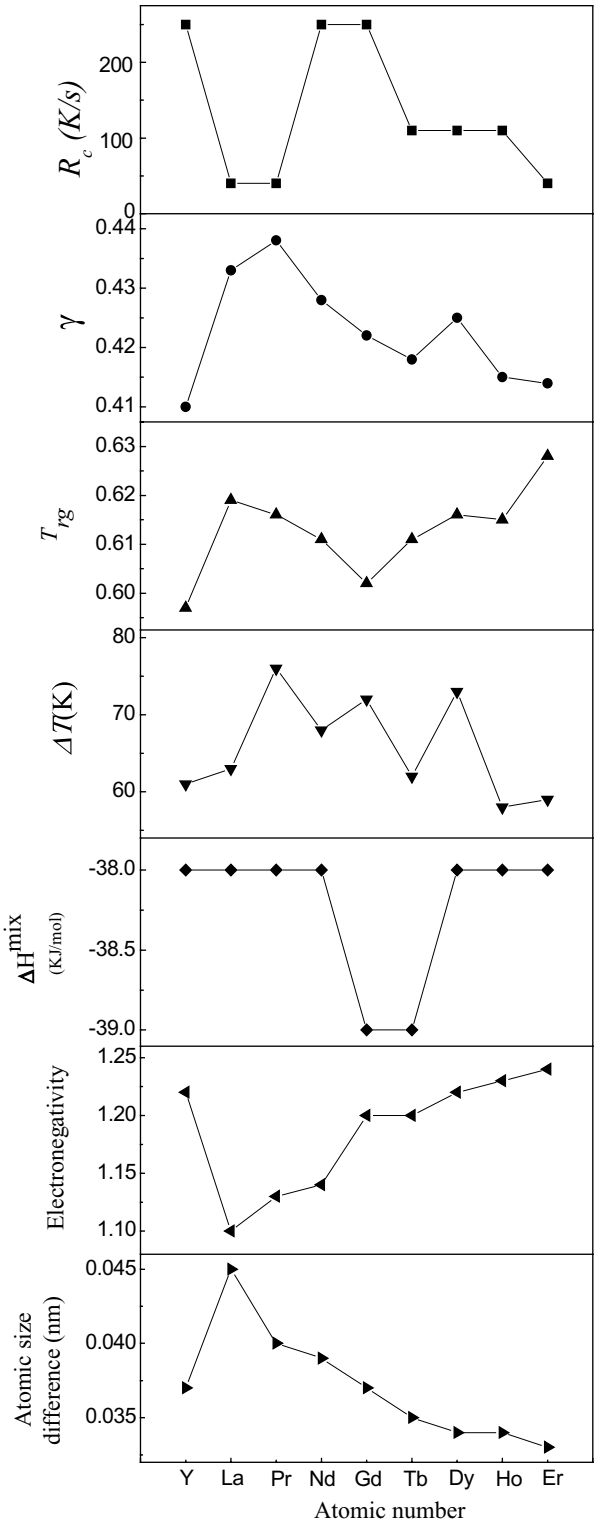

Fig. 3. The dependence of R_c and ΔT, T_{rg}, the atomic size difference $\Delta R(R_{RE}–R_{Al})$, the heat of mixing, ΔH^{mix}(RE–Al) and electronegativity on the atomic number of RE element of the as-cast $RE_{55}Al_{25}Co_{20}$ alloys.

constituent, RE (0.188–0.176 nm), Al (0.143 nm) and Co (0.125 nm), are more than 15%. It can be also found that the GFA of $RE_{55}Al_{25}Co_{20}$ alloys displays the 'V' shape relationship with decreasing atomic radii from La to Er. These results indicate that the large atomic size has significant influence the GFA of the alloys. However, $Ce_{55}Al_{25}Co_{20}$ and $Sm_{55}Al_{25}Co_{20}$ with poor GFA are exceptional.

We note that based on these ternary BMG-forming alloys, novel BMGs with super GFA and unique properties could be obtained via minor addition of other elements such as Y and Co [2,11,15].

3.2. Crystallization, glass transition and fragility of $RE_{55}Al_{25}Co_{20}$ BMGs

Kinetic analysis of crystallization and glass transition of the $RE_{55}Al_{25}Co_{20}$ BMGs were performed by Kissinger's method [24–26]. The activation energy of glass transition (E_g) and crystallization (E_x) of the BMGs are shown in Table 3. Fig. 4(a) and (b) present a rough linear relation between E_g and T_g, E_x and T_x of these BMGs, respectively. The results show a trend that the BMGs with higher $T_g(T_x)$ have larger $E_g(E_x)$. The heavy RE-based alloys have higher thermal stability comparing with that of the light RE-based BMGs.

The fragility can be quantified by the fragility index m defined as [27]

$$m = \left.\frac{\mathrm{d}\log\langle\tau\rangle}{\mathrm{d}\langle T_g/T\rangle}\right|_{T=T_g}, \quad (1)$$

where $\langle\tau\rangle$ is the average relaxation time and T the temperature. The m, which describes how fast the viscosity increases while approaching the structure arrested at T_g, empirically correlates with other properties [14,28–30]. The correlation implies that the underlying mechanism for the glass formation could arise from its liquid behaviors. It has been found that the fragility of glass formers is related to GFA. So it is of important to study the glass formation combining with the liquid behavior of the alloys.

For metallic glasses, the relationship of T_g and $\ln\phi$ can be fitted with Vogel–Fulcher (VF) equation [31],

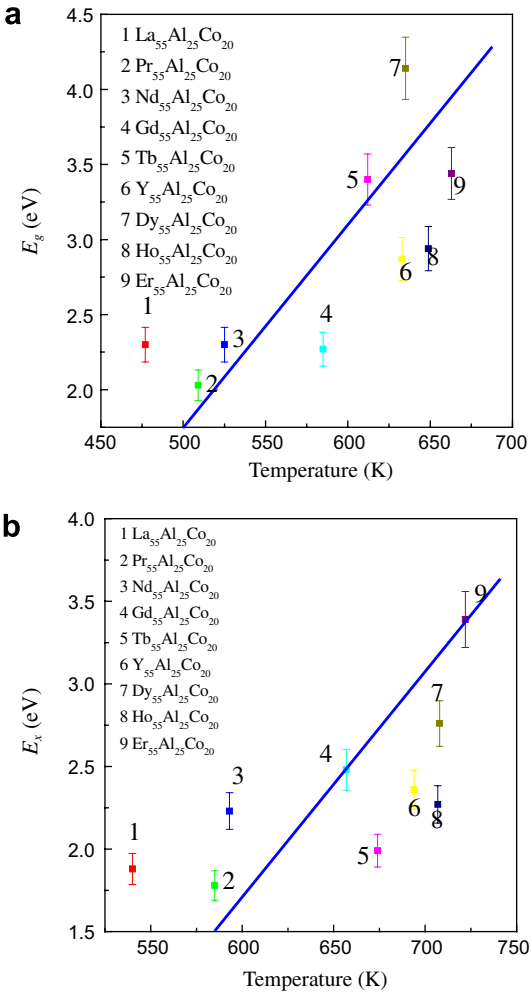

Fig. 4. (a) The linear relation between crystallization activation energy E_x and crystallization temperature T_x of the $RE_{55}Al_{25}Co_{20}$ BMGs. (b) The linear relation between E_g and T_g of the $RE_{55}Al_{25}Co_{20}$ BMGs.

$$\ln\phi = \ln A - \frac{DT_0}{T_g - T_0}, \quad (2)$$

where A is a parameter denoting the time scale in the glass-forming system, D is the strength parameter in the VF

Table 3
The crystallization and glass transition activation energies, fragility m and the fitting parameters $\ln A$, A is a parameter denoting the time scale in the glass-forming system, D (the strength parameter in the VF equation) and VF temperature T_0 and the activation energies of glass transition E_g and of crystallization E_x of the $RE_{55}Al_{25}Co_{20}$ BMGs

Alloys (at.%)	m	$\ln A$	D	T_0 (K)	T_k (K)	E_g (eV)	E_x (eV)
$Y_{55}Al_{25}Co_{20}$	36	6.50	0.169	609	496	2.30	1.88
$La_{55}Al_{25}Co_{20}$	27	9.27	0.723	472	406	2.03	1.78
$Pr_{55}Al_{25}Co_{20}$	38	6.13	0.132	478	350	2.30	2.23
$Nd_{55}Al_{25}Co_{20}$	27	7.31	0.286	501	300	2.27	2.48
$Gd_{55}Al_{25}Co_{20}$	20	34.08	63.71	196	133	3.40	1.99
$Tb_{55}Al_{25}Co_{20}$	32	8.2	0.363	578	555	4.14	2.76
$Dy_{55}Al_{25}Co_{20}$	30	8.06	0.388	591	556	2.94	2.27
$Ho_{55}Al_{25}Co_{20}$	25	10.09	0.953	570	531	3.44	3.39
$Er_{55}Al_{25}Co_{20}$	28	22.95	8.925	449	369	2.87	2.36

Table 4
The density ρ, acoustic velocities (V_l, V_s), elastic constants (Young's modulus E, shear modulus G, Poisson ratio σ and bulk modulus B) compressive strength σ_f, microhardness H_v and Debye temperature θ_D for the $RE_{55}Al_{25}Co_{20}$ BMGs

Alloys (at.%)	ρ (g/cm^2)	V_l (km/s)	V_s (km/s)	E (GPa)	G (GPa)	B (GPa)	σ	θ_D (K)	σ_f (MPa)	H_v (GPa)
$Y_{55}Al_{25}Co_{20}$	4.683	–	–	–	–	–	–	–	1203	4.42
$La_{55}Al_{25}Co_{20}$	5.802	3.213	1.630	40.90	15.42	39.34	0.327	181	989	3.48
$Pr_{55}Al_{25}Co_{20}$	6.373	3.233	1.650	45.90	17.35	43.48	0.324	190	1007	2.58
$Nd_{55}Al_{25}Co_{20}$	6.584	–	–	–	–	–	–	–	996	3.73
$Gd_{55}Al_{25}Co_{20}$	7.343	–	–	–	–	–	–	–	734	4.72
$Tb_{55}Al_{25}Co_{20}$	7.488	3.282	1.747	59.53	22.85	50.19	0.302	203	834	4.42
$Dy_{55}Al_{25}Co_{20}$	7.560	3.325	1.764	61.36	23.52	52.22	0.304	205	717	4.70
$Ho_{55}Al_{25}Co_{20}$	7.888	3.428	1.795	66.64	25.42	58.81	0.311	210	869	4.14
$Er_{55}Al_{25}Co_{20}$	8.157	3.445	1.822	70.72	27.08	60.70	0.306	215	1117	5.45

equation, which controls how closely the liquid system obey the Arrhenius law and T_0 is the asymptotic value of T_g usually approximated as the onset of the glass transition within the limit of infinitely slow cooling and heating rate. The fitting parameters $\ln A$, D and T_0 of $RE_{55}Al_{25}Co_{20}$ alloys are list in Table 3.

From the VF fit the $m$at T_g can be calculated from

$$m = \frac{DT_0T_g}{(T_g - T_0)^2 \ln 10}. \quad (3)$$

The m of the $RE_{55}Al_{55}Co_{20}$ BMGs calculated at a heating rate of 20 K/min from Eq. (3) are shown in Table 3. The m of the $RE_{55}Al_{55}Co_{20}$ BMGs ranges from 20 to 38. The values of m are similar to that of other BMGs such as Zr-, Fe-, Mg-, and Pd-based BMGs [32,33]. According to the Angell's classification [34], these alloys belong to the intermediate strong family. The relative strong liquid behaviors of the $RE_{55}Al_{55}Co_{20}$ alloys come from their much random packed atomic structures with relatively small amount of free volume and tough chemical short-range ordering [35]. However, it is easy to see that the m of these alloys do not correlate with their GFA, based on results contrasted in Tables 2 and 3.

3.3. Elastic constants and mechanical properties of $RE_{55}Al_{25}Co_{20}$ BMGs

Previous studies have shown that the atomic close-packed configuration of BMGs have a close correlation with the elastic behaviors of the glasses, while the elastic constants are intimately related to physical, mechanical and thermodynamic properties of materials [14]. So elastic constants are apparently important parameters for the general understanding of the structural characteristics, mechanical properties and glass transition in metallic glasses [2,32,33,36–39]. The fracture strength σ_f of an ideal solid is theoretically estimated to be about $E/5 - E/10$ [38]. However, due to the existence of defects such as dislocations in crystalline alloys, there is a rough link between E and σ_f:$E/\sigma_f = 500$–$10\,000$. For various glassy alloys, as the absence of dislocations, there is a relation between E and σ:$E/\sigma = 50$ [39].

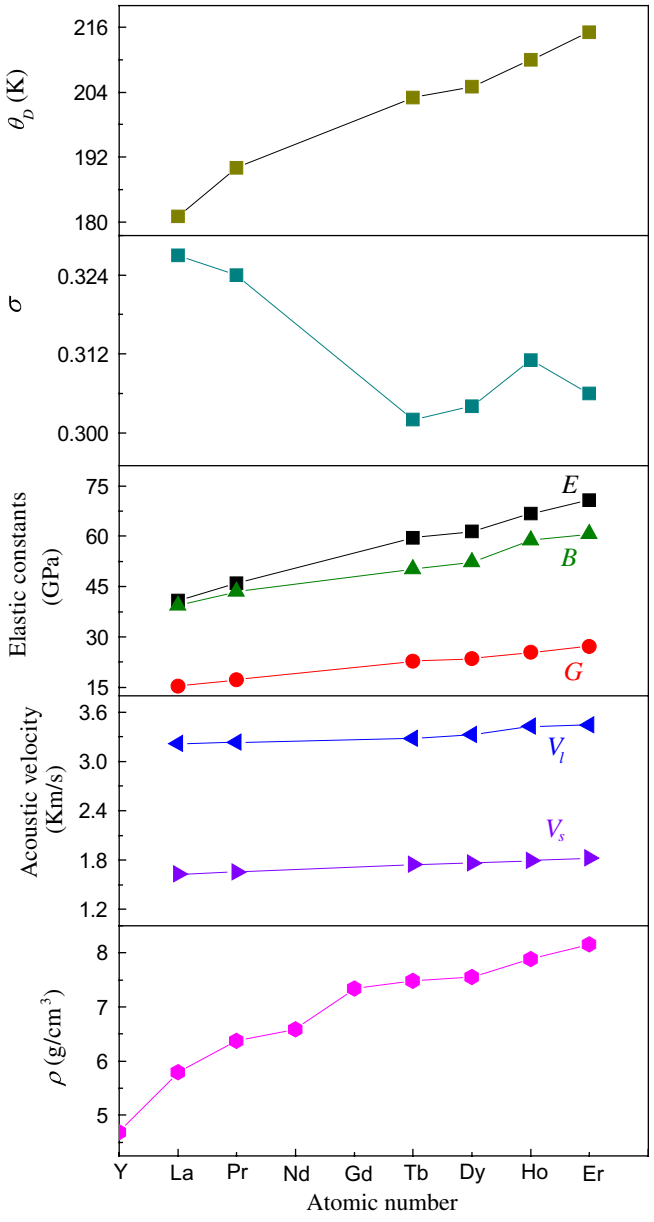

Fig. 5. The dependence of the value of density ρ, V_l, V_s, E, G, B and θ_D on the atomic number of RE elements in the $RE_{55}Al_{25}Co_{20}$ BMGs.

Table 4 lists the density, acoustic velocities, Debye temperature, elastic constants, Vicker's hardness (H_v) and

compression fracture strength (σ_f) for $RE_{55}Al_{25}Co_{20}$ BMGs. θ_D at ambient temperature can be also represented as [21]

$$\theta_D = \frac{h}{k_B}\left(\frac{4\pi}{9}\right)^{-1/3}\rho^{1/3}\left(\frac{1}{v_l^3}+\frac{2}{v_s^3}\right)^{-1/3}, \quad (4)$$

where k_B is the Boltzmann constant, h is the Planck constant and ρ is the density [21].

As shown in Table 4 and Fig. 5, the values of ρ, v_l, v_s, E, G, B and θ_D of the BMG increase with increasing atomic number of RE element (or the increasing elastic moduli of the RE element). The results indicate that the increasing density and elastic constants, θ_D of these alloys can be mainly attributed to the difference of RE elements. It has been found that ductile and brittle behaviors of metallic glasses correlate strongly with σ [40]. The similar low values of σ for $RE_{55}Al_{25}Co_{20}$ BMGs show brittle fracture behavior at room temperature of these BMGs. Fig. 6(a–c) exhibit the relation between fracture strength σ_f and E, H_v and E and H_v and σ_f for $RE_{55}Al_{25}Co_{20}$ BMGs, respectively. As shown in Fig. 6(b), there is a correlation of $E/H_v \approx 10$ for $RE_{55}Al_{25}Co_{20}$ BMGs. However, there are no clear correlations among H_v and σ_f and E and σ_f as indicated in Fig. 6(a) and (c).

Novikov et al. have suggested the existence of a correlation between melt fragility and the B/G (or Poisson's ratio σ) of the glassy materials [41]. The fragility m is plotted versus B/G (or Poisson's ratio σ) in Fig. 7 for $RE_{55}Al_{25}Co_{20}$ BMGs. The correlation between m and B/G appears less stringent than expected. Fig. 8 shows the dependence of T_g on the θ_D for $RE_{55}Al_{25}Co_{20}$ BMGs. The θ_D increases gradually with increasing T_g. Wang et al. suggested that the value of 1000 $T_g/A\theta_D^2$ in BMGs is close to a constant (where A is the average atomic weight), which is within 0.136–0.153 [42]. For the $RE_{55}Al_{25}Co_{20}$ BMGs, the values of 1000 $T_g/A\theta_D^2$ are between 0.130 and 0.153 further confirming the correlation between T_g and θ_D. This correlation means that the glass transition has certain characteristic of melting. Fig. 9 shows the correlation between T_g and elastic constants of the $RE_{55}Al_{25}Co_{20}$ BMGs. The linearly increase trend of T_g with increasing elastic moduli indicating a clear correlation between the thermal stability with their elastic moduli of the BMGs. Because there are good correlations between elastic modulus and hardness, elastic modulus and strength, the hardness and strength can be empirical expressed in terms of T_g [14]. The higher value of T_g indicates higher strength and hardness of a BMG. The positive correlation between the GFA and the strong nature of liquid has been recently suggested [29,43–45]. Fig. 10 plots R_c^{-1} against m of $RE_{55}Al_{25}Co_{20}$ BMGs. It can be seen that there is no an evident positive correlation between them for $RE_{55}Al_{25}Co_{20}$ BMGs. For example, although the $La_{55}Al_{55}Co_{20}$, $Pr_{55}Al_{55}Co_{20}$ and $Er_{55}Al_{55}Co_{20}$ alloys, with markedly different values of m, show the same GFA. The $Nd_{55}Al_{55}Co_{20}$ and $Gd_{55}Al_{55}Co_{20}$ alloys with relative low GFA have lower m value compared to that of

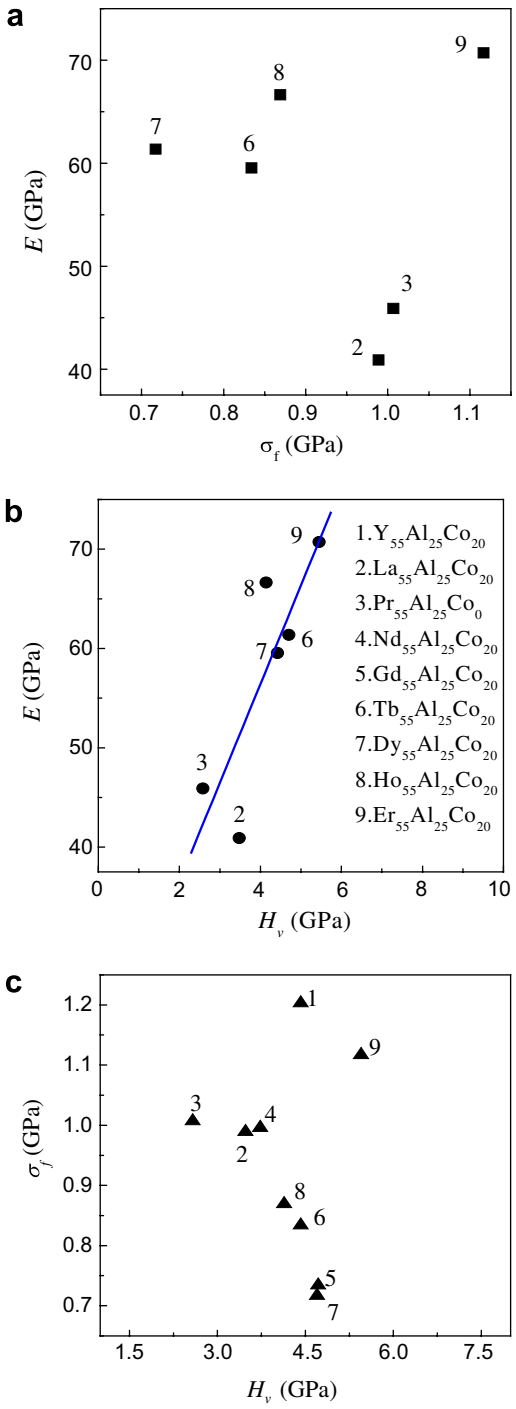

Fig. 6. (a) The correlation of mechanical strength σ_f with elastic modulus E for $RE_{55}Al_{25}Co_{20}$ BMGs. (b) The correlation of Vicker's hardness H_v and E for $RE_{55}Al_{25}Co_{20}$ BMGs. (c) The correlation of H_v and σ_f for $RE_{55}Al_{25}Co_{20}$ BMGs.

$La_{55}Al_{55}Co_{20}$ alloy. On the other hand, the m values of these alloys are much lower than those of $Pd_{43}Ni_{10}Cu_{27}P_{20}$, Vit1 and Vit4 BMGs, while the Pd- and Zr-based alloys show the best GFA among the known BMG-forming systems so far. This indicates that the glass formation in multicomponent alloy is complicated and determined by various factors involved in structural, thermodynamic

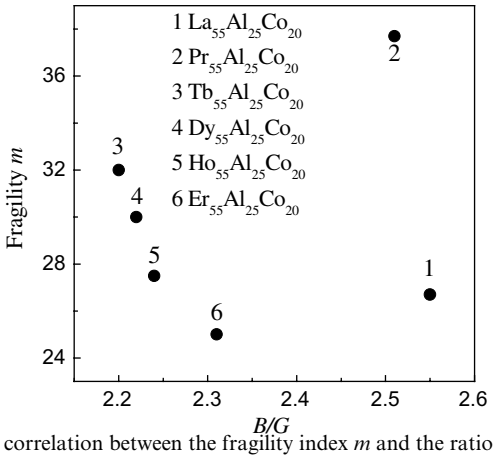

Fig. 7. The correlation between the fragility index m and the ratio of bulk to shear modulus, B/G for $RE_{55}Al_{25}Co_{20}$ BMGs.

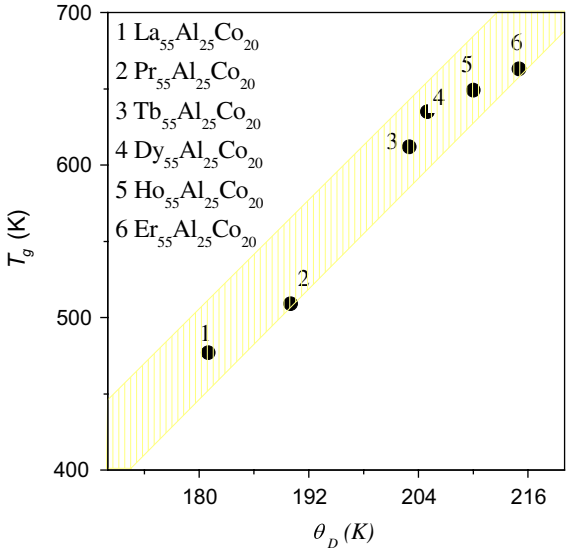

Fig. 8. The correlation between T_g and Debye temperature θ_D for $RE_{55}Al_{25}Co_{20}$ BMGs.

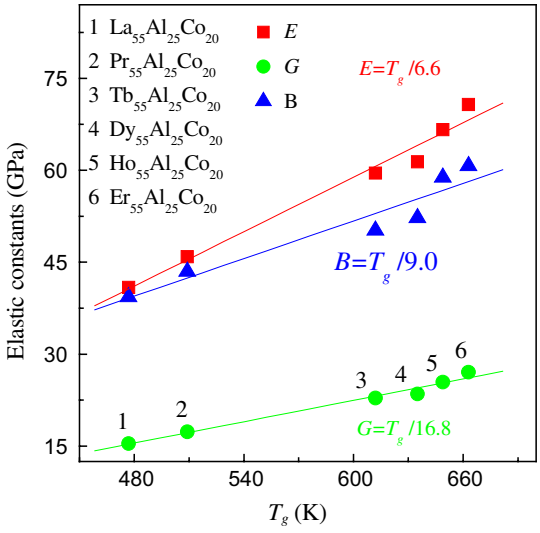

Fig. 9. The correlation between T_g and elastic constants of $RE_{55}Al_{25}Co_{20}$ BMGs.

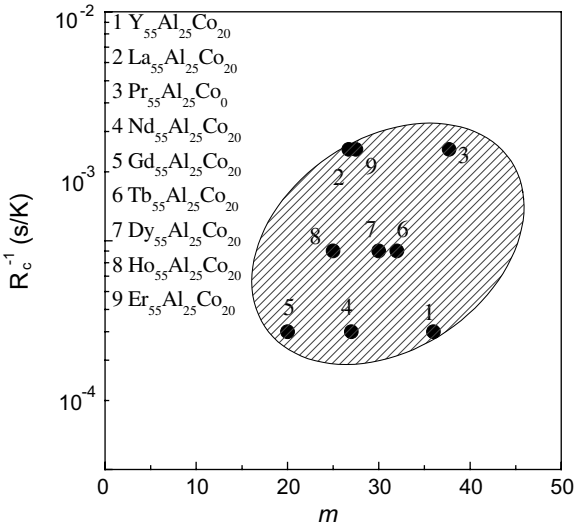

Fig. 10. The correlation of the inverse of the critical cooling rate R_c^{-1} with the fragility index m.

and kinetic aspects. There might be no certain factor that is crucial for the glass formation. To explicitly elucidate the BMG formation mechanism, more works are needed.

4. Summary

A new series of $RE_{55}Al_{25}Co_{20}$ alloys with good GFA is fabricated in bulk form. These BMGs are model systems to investigate the GFA, glass transition, thermal stability, crystallization behavior, elastic constants, mechanical properties and Dedye temperature and review the relationship between these characteristics and properties in the BMGs as a result of their chemical comparability, well-regulated changing atomic size, electronic structure, density and elastic constants of the base RE element. Based on the ternary BMG-forming alloys, new BMG materials can be developed via minor addition approach. The results might be helpful for the understanding of the formation mechanism of metallic glasses and useful for development of more rare earth based BMGs.

Acknowledgement

The financial support of the National Natural Science Foundation of China (Grant No: 50621061) is appreciated.

References

[1] A. Inoue, Acta Mater. 48 (2000) 279.
[2] W.H. Wang, Prog. Mater. Sci. 53 (2007) 540;
W.H. Wang, C. Dong, C.H. Shek, Mater. Sci. Eng. R 44 (2004) 45.
[3] H.S. Chen, Acta Metall. 22 (1974) 1505.
[4] F.Q. Guo, S.J. Poon, G.J. Shiflet, Appl. Phys. Lett. 83 (2003) 2575.
[5] H. Tanaka, J. Non-Cryst. Solids 351 (2005) 678.
[6] O.N. Senkov, D.B. Miracle, H.M. Mullens, J. Appl. Phys. 97 (2005) 103502.
[7] A.L. Greer, Nature 366 (1993) 303.

[8] A. Inoue, T. Zhang, T. Masumoto, Mater. Trans., JIM 31 (1990) 177.
[9] Z.P. Lu, C.T. Liu, Acta Mater. 50 (2002) 3501.
[10] A.L. Drehman, A.L. Greer, D. Turnbull, Appl. Phys. Lett. 41 (1982) 716.
[11] B. Zhang, R.J. Wang, D.Q. Zhao, M.X. Pan, W.H. Wang, Phys. Rev. B 73 (2006) 027609;
Y.X. Wei, M.X. Pan, W.H. Wang, Scripta Mater. 54 (2006) 599;
X.K. Xi, S. Li, R.J. Wang, M.X. Pan, W.H. Wang, J. Mater. Res. 20 (2005) 2243;
Q. Luo, R.J. Wang, M.X. Pan, W.H. Wang, Appl. Phys. Lett. 88 (2006) 181909;
G.J. Fan, W. Löser, J. Eckert, L. Schultz, Appl. Phys. Lett. 75 (1999) 2984.
[12] A. Inoue, N. Nishiyama, T. Masumoto, Mater. Trans., JIM 33 (1992) 937;
J. Shen, Q.J. Chen, J.F. Sun, H.B. Fan, G. Wang, Appl. Phys. Lett. 86 (2005) 151907;
H. Ma, L.L. Shi, J. Xu, Y. Li, E. Ma, Appl. Phys. Lett. 87 (2005) 181915.
[13] A. Peker, W.L. Johnson, Appl. Phys. Lett. 63 (1993) 2342;
L. Xia, Y.D. Dong, Appl. Phys. Lett. 99 (2006) 026103.
[14] W.H. Wang, J. Appl. Phys. 99 (2006) 093506;
J.J. Lewandowski, W.H. Wang, A.L. Greer, Philos. Mag. Lett. 85 (2005) 77;
B. Yang, C.T. Liu, T.G. Nieh, Appl. Phys. Lett. 88 (2006) 221911;
W.L. Johnson, K. Samwer, Phsy. Rev. Lett. 95 (2005) 195501;
H.W. Zhang, G. Subhash, X.N. Jing, L.J. Kecsks, R.J. Dowding, Philos. Mag. Lett. 86 (2006) 333;
W.H. Wang, Z.X. Bao, Phys. Rev. B 61 (2000) 3166.
[15] W.H. Wang, Z. Bian, M.X. Pan, D.Q. Zhao, Intermetallics 10 (2002) 1249;
Z.P. Lu, C.T. Liu, J. Mater. Sci. 39 (2004) 3965.
[16] Z.F. Zhao, D.Q. Zhao, W.H. Wang, Appl. Phys. Lett. 82 (2003) 4699.
[17] B. Zhang, M.X. Pan, W.H. Wang, Appl. Phys. Lett. 85 (2004) 61.
[18] M.B. Tang, D.Q. Zhao, W.H. Wang, J. Phys. D: Appl. Phys. 37 (2004) 973.
[19] Y. He, C.E. Price, S.J. Poon, G.J. Shiflet, Philos. Mag. Lett. 70 (1994) 371.
[20] W.H. Wang, R.J. Wang, M.X. Pan, Appl. Phys. Lett. 74 (1999) 1803.
[21] D. Schreiber, Elastic Constants and Measurement, McGraw-Hill, NY, 1973, p. 35.
[22] W.L. Johnson, JOM 54 (2002) 40.
[23] X.H. Lin, W.L. Johnson, J. Appl. Phys. 78 (1995) 6514.
[24] H.E. Kissinger, J. Res. Natl. Bur. Stand. 57 (1956) 217.
[25] S. Li, R.J. Wang, M.X. Pan, D.Q. Zhao, W.H. Wang, Scripta Mater. 53 (2005) 1489.
[26] B. Zhang, R.J. Wang, M.X. Pan, D.Q. Zhao, W.H. Wang, Phys. Rev. B 70 (2004) 224208.
[27] R. Böhmer, C.A. Angell, Phys. Rev. B 45 (1992) 10091.
[28] L.M. Martinez, C.A. Angell, Nature 410 (2001) 663.
[29] R. Busch, E. Bakke, W.L. Johnson, Acta Mater. 46 (1998) 4725.
[30] L. Battezzati, Mater. Trans. 46 (2005) 2915;
G.P. Johari, Philos. Mag. 86 (2006) 1567.
[31] R. Brüning, K. Samwer, Phys. Rev. B 46 (1992) 11318.
[32] W.L. Johnson, Mater. Res. Bull. 24 (1999) 42.
[33] A. Inoue, Mater. Trans. 43 (2002) 1892.
[34] C.A. Angell, Science 267 (1995) 1924.
[35] Z. Zhang, R.J. Wang, B.C. Wei, W.H. Wang, Appl. Phys. Lett. 81 (2002) 4371.
[36] J.C. Dyre, Nature Mater. 3 (2004) 749.
[37] B. Lawn, Fracture of Brittle Solids, Cambridge University, Cambridge, 1993.
[38] A.L. Greer, Science 267 (1995) 1947.
[39] W.H. Wang, J. Non-Cryst. Solids 351 (2005) 1481.
[40] T. Egami, Intermetallics 14 (2006) 882.
[41] V.N. Novikov, A.P. Sokolov, Nature 431 (2004) 961.
[42] W.H. Wang, P. Wen, D.Q. Zhao, M.X. Pan, R.J. Wang, J. Mater. Res. 18 (2003) 2747.
[43] D.N. Perera, J. Phys.: Condens. Matter. 11 (1999) 3807.
[44] Z.P. Lu, Y. Li, C.T. Liu, J. Appl. Phys. 93 (2003) 286.
[45] B. Zhang, R.J. Wang, M.X. Pan, D.Q. Zhao, W.H. Wang, Acta Mater. 54 (2006) 3025.